Magnitude and phase of three-dimensional (3D) velocity vector: Application to measurement of cochlear promontory motion during bone conduction sound transmission

Dobrev, Ivo ; Sim, Jae Hoon

Abstract: Recent measurements of vibrational motion to assess sound transmission through ear structures and skull contents have included three-dimensional (3D) behavior. The 3D motion of a point has been described with the three orthogonal components in the 3D space. In this article, a method to represent the 3D velocity with the magnitude and phase of the resultant velocity is introduced. This method was applied to the measurement of cochlear promontory motion as an indication of bone conduction (BC) sound transmission. The promontory motions were measured on the ipsilateral and contralateral sides, and the transcranial attenuation and phase delay of the contralateral side relative to the ipsilateral side were calculated. The transcranial attenuation and phase delay calculated with the maximum magnitudes and corresponding phases of the resultant were a better fit to the interaural threshold difference and transcranial time interval between the ipsilateral and contralateral sides as reported in the literature, than the attenuation and phase delay calculated with any individual Cartesian motion component.

DOI: https://doi.org/10.1016/j.heares.2018.03.022

Originally published at:
Dobrev, Ivo; Sim, Jae Hoon (2018). Magnitude and phase of three-dimensional (3D) velocity vector: Application to measurement of cochlear promontory motion during bone conduction sound transmission. Hearing Research, 364:96-103.
DOI: https://doi.org/10.1016/j.heares.2018.03.022

Magnitude and Phase of Three-Dimensional (3D) Velocity Vector:

Application to measurement of cochlear promontory motion during bone conduction sound transmission

Ivo Dobrev and Jae Hoon Sim

Department of Otorhinolaryngology, Head and Neck Surgery, University Hospital Zurich

Hearing Research: accepted and in press (https://doi.org/10.1016/j.heares.2018.03.022)

Highlights

- A method to calculate the magnitude and phase of the 3D velocity vector is described.
- The 3D velocity of a point can be represented by the magnitude and phase of the resultant instead of the magnitudes and phases of the three orthogonal components.
- The method was applied to the measurement of cochlear promontory motion as an indication of bone conduction (BC) sound transmission.
- The maximum velocity vector of the cochlear promontory motion is a better descriptor of BC hearing than individual Cartesian components.

Abstract

Recent measurements of vibrational motion to assess sound transmission through ear structures and skull contents have included three-dimensional (3D) behavior. The 3D motion of a point has been described with the three orthogonal components in the 3D space. In this article, a method to represent the 3D velocity with the magnitude and phase of the resultant velocity is introduced. This method was applied to the measurement of cochlear promontory motion as an indication of bone conduction (BC) sound transmission. The promontory motions were measured on the ipsilateral and contralateral sides, and the transcranial attenuation and phase delay of the contralateral side relative to the ipsilateral side were calculated. The transcranial attenuation and phase delay calculated with the maximum magnitudes and corresponding phases of the resultant were a better fit to the interaural threshold difference and transcranial time interval between the ipsilateral and contralateral sides as reported in the literature, than the attenuation and phase delay calculated with any individual Cartesian motion component.

Introduction

Vibrational motions have been measured to assess sound transmission through the ear structures and skull contents in normal and reconstructed middle ears, for both air conduction (AC) and bone conduction (BC) stimulation. For example, motions of the stapes are frequently measured together with the ear-canal pressure to obtain the middle-ear transfer function (METF) for transmission of AC sound via the middle ear; vibrations of the cochlear promontory are measured assuming that it reflects transmission of BC sound to the cochlea and can thus predict the BC stimulation required to induce hearing sensations (Stenfelt and Goode 2005; Eeg-Olofsson et al. 2008). Measurements of the vibrational motions of the ear structures were made in a one-dimensional (1D) manner in the early stages and were later extended to include three-dimensional (3D) behavior. Laser Doppler vibrometry (LDV) systems are one of the standard tools used to measure small vibrations of the ear structures, and 3D measurements are typically based on a method introduced by Decraemer et al. (1994). They mounted temporal bones on two stacked goniometers and measured velocities at a point on the middle-ear ossicles using an LDV system with several different laser beam angles that were obtained by rotating the two goniometers. Recently, measurement of the three translational components at a specified measurement point has become easier with the development of 3D LDV systems, which have three built-in laser beams with three different measurement angles.

The 3D behavior of a point has generally been described with the three orthogonal components of the motion at the specified point. However, when the 3D components have different phases, they do not show the magnitude and phase of the resultant directly. The magnitude and phase of the resultant may have important meanings in some cases, for example, indication of BC sound transmission by measuring vibration of the cochlear promontory. In this case, we hypothesize that the resultant of the promontory motion rather than any orthogonal component of the promontory motion is a better descriptor of BC hearing. This article describes a method for calculating the magnitude and phase of the resultant from the three orthogonal

motion components. The method was applied to measurements of cochlear promontory motion on the ipsilateral and contralateral sides with excitation by a bone-anchored hearing aid (BAHA) in cadaver heads. The transcranial attenuation and phase delay of the contralateral side relative to the ipsilateral side were obtained based on the attenuation of the maximum magnitude and phase delay of the resultant. The results were compared with interaural threshold difference between the ipsilateral and contralateral sides and expected transcranial phase delay data reported in the literature.

Rationale

This article provides a way to represent 3D velocity with the magnitude and phase of the resultant, which have been previously described with the three orthogonal components in the Cartesian coordinate system. Such an approach could be useful in cases for which the resultants are presumed to provide a more direct indication of sound transmission, for example measuring vibration of the cochlear promontory to assess transcranial attenuation and phase delay in BC sound transmission.

Description of Method

Representation of 3D velocity vector as its resultant vector

Let's consider a velocity vector **V** of a harmonic motion in the 3D space, which has V_x, V_y and V_z as the *xyz* components. The vector **V** can be written as,

$$\mathbf{V} = V\mathbf{n} = V_x\mathbf{i} + V_y\mathbf{j} + V_z\mathbf{k}\,, \tag{1}$$

where the **i**, **j**, and **k** are the unit vectors in the *x*, *y*, and *z* direction, and **n** is the unit vector in the direction of the vector **V**. Note that the direction of the unit vector **n** changes during a cycle whereas the directions of the **i**, **j**, and **k** are fixed in the 3D space. If the *xyz* components V_x, V_y and V_z have phases of θ_x, θ_y, and θ_z, respectively, at an angular frequency ω, the V_x, V_y and V_z can be represented as a function of time *t* as,

$$\begin{aligned} V_x &= |V_x|\cos(\omega t + \theta_x) \\ V_y &= |V_y|\cos(\omega t + \theta_y). \\ V_z &= |V_z|\cos(\omega t + \theta_z) \end{aligned} \tag{2}$$

Then,

$$V^2 = V(t)^2 = |V_x|^2\cos^2(\omega t + \theta_x) + |V_y|^2\cos^2(\omega t + \theta_y) + |V_z|^2\cos^2(\omega t + \theta_z) \tag{3}$$

By applying a formula $\cos^2\alpha = \dfrac{\cos 2\alpha + 1}{2}$,

$$V(t)^2 = \frac{1}{2}\left[|V_x|^2 + |V_y|^2 + |V_z|^2 + |V_x|^2\cos 2(\omega t + \theta_x) + |V_y|^2\cos 2(\omega t + \theta_y) + |V_z|^2\cos 2(\omega t + \theta_z)\right]. \tag{4}$$

By applying another formula $\cos(\alpha + \beta) = \cos\alpha\cos\beta - \sin\alpha\sin\beta$,

$$V(t)^2 = \frac{1}{2}\left[|V_x|^2 + |V_y|^2 + |V_z|^2 + A\cos 2\omega t - B\sin 2\omega t\right] \tag{5}$$

with

$$\begin{aligned} A = {} & |V_x|^2\cos 2\theta_x + |V_y|^2\cos 2\theta_y + |V_z|^2\cos 2\theta_z \\ B = {} & |V_x|^2\sin 2\theta_x + |V_y|^2\sin 2\theta_y + |V_z|^2\sin 2\theta_z \end{aligned}$$

The last two terms in Eq. (5) can be combined as follows:

$$V(t)^2 = \frac{1}{2}\left[|V_x|^2 + |V_y|^2 + |V_z|^2 + \sqrt{A^2 + B^2}\cos 2(\omega t + \varphi)\right] \tag{6}$$

with

$$\cos 2\varphi = \frac{A}{\sqrt{A^2 + B^2}},\ \sin 2\varphi = \frac{B}{\sqrt{A^2 + B^2}},\ \tan 2\varphi = \frac{B}{A}. \tag{7}$$

Since $\sqrt{A^2 + B^2}\cos 2(\omega t + \varphi)$ has the magnitude of $\sqrt{A^2 + B^2}$, the maximum magnitude $|V|_{MAX}$ of the spatial velocity vector **V** can be obtained as,

$$|V|_{MAX} = \sqrt{\frac{1}{2}\left[|V_x|^2 + |V_y|^2 + |V_z|^2 + \sqrt{A^2 + B^2}\right]}. \tag{8}$$

Consequently, the minimum magnitude $|V|_{MIN}$ of the spatial velocity vector **V** becomes,

$$|V|_{MIN} = \sqrt{\frac{1}{2}\left[|V_x|^2 + |V_y|^2 + |V_z|^2 - \sqrt{A^2 + B^2}\right]}. \tag{9}$$

The phase φ of the spatial velocity vector **V** can be calculated from Eq. (7). Note that two values for φ are obtained from Eq. (7). That is, once 2φ is calculated in the range of $-\pi < 2\varphi \le \pi$ using Eq. (7), then, the two solutions for φ are:

$$\varphi_1 = (2\varphi)/2 \text{ and } \varphi_2 = (2\varphi)/2 + \pi. \tag{10}$$

Since the phase is calculated from the square of the velocity in Eq. (6), two phases with a difference of π are obtained for two opposite directions. That is, the unit vector $\mathbf{n}_P$**,** which represents the direction of the maximum magnitude of the vector **V,** can be defined in either of two opposite directions, and the phase is determined by choice of the direction of the maximum magnitude. Considering the fact that **V** has its positive maximum at $\omega t = -\varphi$, the two unit vectors $\mathbf{n}_{P1}$ and $\mathbf{n}_{P2}$ for φ_1 and φ_2 can be obtained by,

$$\mathbf{n}_{P1} = \frac{1}{|V|_{MAX}} \begin{Bmatrix} |V_x| \cos(-\varphi_1 + \theta_x) \\ |V_y| \cos(-\varphi_1 + \theta_y) \\ |V_z| \cos(-\varphi_1 + \theta_z) \end{Bmatrix} \text{ and } \mathbf{n}_{P2} = \frac{1}{|V|_{MAX}} \begin{Bmatrix} |V_x| \cos(-\varphi_2 + \theta_x) \\ |V_y| \cos(-\varphi_2 + \theta_y) \\ |V_z| \cos(-\varphi_2 + \theta_z) \end{Bmatrix}. \quad (11)$$

In Eq. (11), $\frac{1}{|V|_{MAX}}$ scales the magnitude of the directional vectors $\mathbf{n}_{P1}$ and $\mathbf{n}_{P2}$ to a unit. Since the phase of the minimum magnitude is obtained by adding π/2 to the phase of the maximum magnitude, the two unit vectors $\mathbf{n}_{Q1}$ and $\mathbf{n}_{Q2}$ for the minimum magnitude can be obtained by,

$$\mathbf{n}_{Q1} = \frac{1}{|V|_{MAX}} \begin{Bmatrix} |V_x| \cos(-\varphi_1 + \pi/2 + \theta_x) \\ |V_y| \cos(-\varphi_1 + \pi/2 + \theta_y) \\ |V_z| \cos(-\varphi_1 + \pi/2 + \theta_z) \end{Bmatrix} \text{ and } \mathbf{n}_{P2} = \frac{1}{|V|_{MAX}} \begin{Bmatrix} |V_x| \cos(-\varphi_2 + \pi/2 + \theta_x) \\ |V_y| \cos(-\varphi_2 + \pi/2 + \theta_y) \\ |V_z| \cos(-\varphi_2 + \pi/2 + \theta_z) \end{Bmatrix}. \quad (12)$$

Figure 1 illustrates the trajectory of a 3D velocity vector **V** with the two points of the maximum magnitude (*P*1 and *P*2) and the two points of the minimum magnitude (*Q*1 and *Q*2) during a cycle. Note that the two unit vectors $\mathbf{n}_{P1}$ and $\mathbf{n}_{P2}$ in the directions of the maximum magnitude are in opposite directions from each other (i.e., $\mathbf{n}_{P2} = -\mathbf{n}_{P1}$), and so are the two unit vectors $\mathbf{n}_{Q1}$ and $\mathbf{n}_{Q2}$ indicating the directions of the minimum magnitude.

While the trajectory generally has a shape of an ellipse, the trajectory has a shape of a straight line (i.e., the 3D velocity vector **V** becomes one-dimensional) or s circle (i.e., the magnitude of the 3D velocity vector **V** is constant during a cycle) for some cases.

In order for the trajectory to become a straight line, the minimum magnitude of the 3D velocity vector **V** should have zero value ($|V|_{MIN} = 0$,) and from Eq. (9), it results in

$$|V_x|^2 + |V_y|^2 + |V_z|^2 = \sqrt{A^2 + B^2}\,. \quad (13)$$

By squaring both sides of Eq. (13), we obtain,

$$
\begin{aligned}
&|V_x|^2|V_y|^2\left(1-\cos 2\theta_x \cos 2\theta_y - \sin 2\theta_x \sin 2\theta_y\right) \\
&+|V_y|^2|V_z|^2\left(1-\cos 2\theta_y \cos 2\theta_z - \sin 2\theta_y \sin 2\theta_z\right) \\
&+|V_z|^2|V_x|^2\left(1-\cos 2\theta_z \cos 2\theta_x - \sin 2\theta_z \sin 2\theta_x\right)=0
\end{aligned} \tag{14}
$$

With formulas $\cos\alpha\cos\beta = \dfrac{\cos(\alpha+\beta)+\cos(\alpha-\beta)}{2}$ and $\sin\alpha\sin\beta = \dfrac{\cos(\alpha-\beta)-\cos(\alpha+\beta)}{2}$,

Eq. (14) is simplified as,

$$
|V_x|^2|V_y|^2\left\{1-\cos 2(\theta_x-\theta_y)\right\}+|V_y|^2|V_z|^2\left\{1-\cos 2(\theta_y-\theta_z)\right\}+|V_z|^2|V_x|^2\left\{1-\cos 2(\theta_z-\theta_x)\right\}=0 \tag{15}
$$

From Eq. (15), if the phases θ_x, θ_y, and θ_z of the *xyz* components are the same or have π difference each other, $|V|_{MIN}=0$ and thus the trajectory becomes a straight line, independently of the magnitude of the *xyz* components.

In order for the trajectory to have a circular shape, the magnitude of the 3D velocity vector **V** should be constant during a cycle, and from Eq. (6), it results in $A^2+B^2=0$. That is,

$$
\left(|V_x|^2\cos 2\theta_x+|V_y|^2\cos 2\theta_y+|V_z|^2\cos 2\theta_z\right)^2+\left(|V_x|^2\sin 2\theta_x+|V_y|^2\sin 2\theta_y+|V_z|^2\sin 2\theta_z\right)^2=0. \tag{16}
$$

Eq. (16) can be simplified as,

$$
|V_x|^4+|V_y|^4+|V_z|^4+2|V_x|^2|V_y|^2\cos 2(\theta_x-\theta_y)+2|V_y|^2|V_z|^2\cos 2(\theta_y-\theta_z)+2|V_z|^2|V_x|^2\cos 2(\theta_z-\theta_x)=0 \tag{17}
$$

Eq. (17) is satisfied, for example, in the case that $|V_x| = |V_y|$, $|V_z| = 0$, and. $\theta_x - \theta_y = \frac{\pi}{2}$ However, a condition of the phases of the *xyz* components that satisfies Eq. (17) independently of the magnitudes of the *xyz* components does not exist.

Now, choice of the phase of the velocity vector **V** among two possible phases of φ_1 and φ_2 is of concern. Two suggestions can be provided for choice of the phase of the velocity vector **V**:

1) Choose either of two possible phases arbitrarily at a specific frequency. Then, at the adjacent frequency, choose the phase such that the direction of the corresponding positive maximum changes with a smaller angle from the direction of the positive maximum at the previous frequency. In this case, a sufficiently small frequency step is necessary.
2) The side of the positive maximum can be defined anatomically. For example, when sound wave propagation on the skull surface with bone conduction stimulation is measured (Dobrev et al. 2017), either of outward side or inward side of the skull surface can be chosen as the side of the positive maximum consistently through the considered frequency range.

Measurement of cochlear promontory motion during bone conduction sound transmission

The cochlear promontory motions of the ipsilateral and contralateral sides were measured in four cadaver heads with stimulation using a BAHA transducer. A BAHA Cordelle II (Cochlear AG, Australia) transducer was placed on the mastoid (5 cm behind the external auditory canal opening) using a 5-Newton steel headband (BAHA headband 90138, Cochlear AG, Australia), and the coupling force was maintained at approximately 5 Newtons (Dobrev et al 2016).

The cadaver heads were positioned in a natural upright position. A metal rod of 12-mm diameter was inserted in the remaining spinal column (~5 cm) of the cadaver head, and the metal rod was mounted on the vibration-isolation table (M-INT1-36-6-A, Newport Corp., CA, USA) with vibration-isolation legs (sorbothane legs, AV3, Thorlabs Inc., NJ, USA). Additional support with rubber bands was made for horizontal stability of the cadaver heads. Four tensional forces spaced by 90 degrees were made horizontally by four rubber bands, which are supported by four metal rods on the vibration-isolation table and are connected to four points of the cadaver head via a BAHA Softband (Cochlear AG, Australia) on the cadaver head, at approximately 2-cm above the pinna.

The BAHA transducer was driven sequentially by 81 stepped sine signals, distributed logarithmically in the frequency range of 0.1 to 10 kHz, resulting in approximately 40 frequency points per decade. An endaural incision between the helix and tragus was performed, and tympanomeatal flap was elevated, to expose the cochlear promontory (Fisch 2008; Huber et al. 2013). The cochlear promontory motions near the round window (2-4 mm from the boundary of the round window) were measured using a 3D laser Doppler vibrometry (3D LDV) system (CLV-3D, Polytec GmbH, Germany). The 3D LDV system was positioned such that the laser beam was oriented along the lateral-medial direction. The signal generation and velocity measurement were handled via a data acquisition system (APx585, Audio Precision Inc., USA), with a sampling frequency of 96 kHz and sampling time of 200 ms. The measurement at each frequency was repeated five times, and the five measurements were recorded as complex numbers to represent the magnitude and phase. Then, the median value across the five measurements was taken for each of the real and imaginary parts of the data for further analysis.

Results and Discussion

The vector with the maximum magnitude and the corresponding direction is defined as the maximum velocity vector in the remaining parts of this article, for convenience.

Figure 2 displays trajectories of velocities of the cochlear promontory on the ipsilateral (red) and contralateral (blue) sides during one cycle, at 0.25, 0.5, 1, 2, 4, and 8 kHz in one cadaver head (CH1). The positive *x*-, *y*- and *z*- directions indicate the anterior, superior, and lateral directions, respectively (A right-handed frame system was used for the right side, and a left-handed frame system for the left side, to maintain the same positive directions in both sides). The spheres at each trajectory indicate the points of the maximum magnitude. The direction of the maximum velocity vector varied significantly with frequency for both the ipsilateral and contralateral sides. For example, for both sides, the z-component was dominant at 0.25 kHz but

was relatively small at 8 kHz. The directions of the maximum velocity vector on both sides were similar for some frequencies (for example, 8 kHz) and quite different for others (for example, 0.5 kHz). The trends of CH1 shown in Fig. 2 was not maintained in other cadaver heads. The frequency dependent change of the direction was different across the cadaver heads, without a clear pattern. The difference of the maximum magnitude between the ipsilateral and contralateral sides did not show consistent patterns across the cadaver heads.

Figure 3 illustrates the maximum magnitudes (dotted black) in comparison with the magnitudes of the x- (red), y- (green), and z- (blue) components for the ipsilateral (upper) and contralateral (bottom) sides, in each cadaver head. The figure clearly shows that the largest component among the x, y, and z components differed with frequency, and the maximum magnitudes were beyond the magnitudes of the largest component. In the case that one component is dominant compared to other components, the magnitude of the maximum magnitude was similar to the dominant component (for example, the x-component at high frequencies in CH1 and CH4 and the z-component at low frequencies in CH1 and CH3, on the ipsilateral side). Additionally, while the individual orthogonal components exhibited steep (slopes > 30dB/octave) notches, varying between heads and sides, the maximum magnitudes indicated a clear and monotonous trend, typically observed in audiometric tests of BC hearing thresholds.

In Figure 4, the phase of the maximum velocity vector (dotted black) in comparison with the phases of the x- (red), y- (green), and z- (blue) components for the ipsilateral (upper) and contralateral (bottom) sides are shown. On the ipsilateral side, the phase of the maximum velocity vector was similar with all the velocity components in CH1, CH2, and CH3, and with the z-component (component in the lateral direction), at low frequencies below 300 Hz. At higher frequencies, the phase of the maximum velocity vector was similar to the y-component (component in the superior direction) in CH2 and the x-component (component in the anterior direction) in CH3. At the high frequencies, the phase of the maximum velocity vector showed

a half-cycle difference from the x- and z-components in CH1 and CH2 and from the y- and z-components in CH3. In CH4. The phase of the maximum velocity vector showed difference of about a cycle from the x-components above 400 Hz and from the z-component in the frequency range of 0.4-3 kHz. On the contralateral side, the phase of the x-component was similar to the phase of the maximum velocity vector in CH1 and CH2, but showed differences for the low- and mid-frequency range in CH3 and for the mid- and high-frequency range in CH4. The phase of the z-component showed a half-cycle difference from the phase of the maximum velocity vector at low frequencies in all cadaver heads, and was similar to the phase of the maximum velocity vector at mid- and high-frequency range in CH1 and CH2. Similar to the magnitude, the phase of the maximum velocity vector indicated a clearer and more monotonous trend.

Figure 5 illustrates the transcranial attenuation of the promontory motion (i.e., ratio of the promontory motion on the contralateral side to the promontory motion on the ipsilateral side) on a dB scale (upper) and phase delay between the two sides (bottom). The transcranial attenuation and phase delay were calculated with the x-component (red), y-component (green), z-component (blue), and the maximum velocity vector (dotted black). These were compared with interaural differences calculated from audiometric thresholds with stimulation on the mastoid by Ito et al. (2011), and expected phase delay with a transcranial time interval (Δt_{tc}) of 0.3~0.4 ms between the two sides, as reported in the literature (Stenfeld and Goode 2005; McKnight et al. 2013; Sim et al. 2014; Dobrev et al. 2017). The interaural differences from audiometric thresholds in Ito et al. were obtained for each subject, and were averaged across 15 subjects for the mean and standard deviation (The raw data of the audiometric thresholds in Ito et al. were available from the authors of the article). The attenuation calculated from the maximum velocity vector was within the range of one standard deviation (STD) of the interaural threshold difference reported in Ito et al. for all frequencies and in all cadaver heads, except at 0.25 and 0.5 kHz. It is known that the skull shows rigid-body-like motions below 1 kHz (Dobrev et al. 2017), and that such motions would be affected by the mounting conditions. The deviance

at 0.25 and 0.5 kHz is presumed to be due to different mounting conditions between the cadaver heads in this study and the human subjects in the study by Ito et al. The attenuation calculated from the y-component was not consistently within the range, with various notches and peaks. The attenuations calculated from the x- and z-components were generally within the range at the frequencies of the audiometric test, but included various notches and peaks as well. Generally, the phase delays calculated from the maximum velocity vector and the x-component were in better agreement with the expected phase delay from the time interval of 0.3~0.4ms than the phase delays calculated from the y-and z-components. The phase delay calculated from the maximum velocity vector showed some amounts of difference from the expected phase delay in the frequency range of 0.3–1 kHz, but the difference was generally within 0.25 cycles. In other frequency ranges, the phase delay calculated from the maximum velocity vector were in good agreement with the expected delay, except for the frequency range of 2-6 kHz in CH2. The phase delay calculated from the x-components showed a good agreement with the expected phase delay at low frequencies below 300 Hz in CH1 and CH2 and at high frequencies above 1 kHz in CH3 and CH4. The phase delay calculated from the z-components showed a half cycle difference from the expected phase delay at low frequencies in CH1, CH2, and CH3, and were similar with the expected phase delay at high frequencies in CH1, CH2, and CH3.

Figure 6 shows the transcranial attenuation of the promontory motion with the average values and standard deviations across the 4 cadaver heads, in comparison with the interaural threshold difference calculated from the hearing thresholds in 15 subjects in Ito et al. To quantify similarity between the transcranial attenuation of each motion component (across n = 4 samples) and the interaural threshold difference (across n = 15 subjects), the average distance between the two data sets, at the corresponding frequency, was calculated based on the distances (absolute of the difference, in dB) between all possible data pairs (cross-combinations) from the two data sets, for each motion component. The calculated average distance was compared with the standard deviation of the interaural difference, at each frequency, as a metrics of

similarity between each motion component and the clinical data. The average distances with the x-component were 4.9, 7.0, 8.0, and 8.3 dB at 1, 2, 3, and 4 kHz, respectively, and were smaller than the standard deviations of the interaural difference only at 2 kHz. The average distances with the y-component (4.3, 9.9, 14.8, and 8.6 dB at 1, 2, 3, and 4 kHz, respectively) were larger than the standard deviations of the interaural difference for all the frequencies. With the z-component, the average distances (3.1, 6.6, 8.9, and 10.9 dB at 1, 2, 3, and 4 kHz, respectively) were within the standard deviations of the interaural difference at 1 and 2 kHz, and above the standard deviations of the interaural difference at 3 and 4 kHz. With the maximum velocity vector, the average distances were 3.1, 7.3, 6.7, and 6.7 dB at 1, 2, 3, and 4 kHz, respectively, and those values were within the standard deviations of the interaural difference (3.8, 8.3, 7.4, and 7.7 dB at 1, 2, 3, and 4 kHz, respectively). In addition, the transcranial attenuation of the maximum velocity vector had overall smaller standard deviations across samples, along the considered frequency range, than those of other velocity components, making it presumably more consistent metrics across samples.

From the results of this study, assuming that the interaural threshold difference is monotonous without large peaks and notches across the frequencies in Ito et al., it is presumed that the magnitude and phase of the maximum velocity vector of the cochlear promontory motion is a better descriptor of BC hearing than individual orthogonal components of the promontory motion. In addition, considering a fact that the transcranial attenuation based on the maximum velocity has smaller standard deviation than that of any of the individual orthogonal components (across cadaver heads as shown in Fig 6), it is presumed that the required number of samples can be reduced if the BC hearing is assessed with the maximum velocity vector of the cochlear promontory motion.

The method introduced in this article provides a way to represent the 3D velocity at a point with a magnitude and a phase instead of three magnitudes and three phases of the three velocity components in the Cartesian coordinate system. With such an approach, the magnitude

and phase of the maximum velocity vector are determined independently of choice of the Cartesian coordinate system. The method could be useful in cases for which propagation of the vibrational energy is presumed to be meaningful and thus resultants provide a more direct indication of sound propagation, for example measuring vibration of the cochlear promontory to assess transcranial attenuation described in this article and sound wave propagation on the human skull surface (Dobrev et al. 2017), with bone conduction stimulation.

Reference

Decraemer WF, Khanna SM, and Funnell WRJ (1994). A method for determining three-dimensional vibration in the ear. Hearing Research 77(1-2): 19-37.

Dobrev I, Stenfelt S, Roosli R, Lucy Bolt, Gerig R, Pfiffner F, Gerig R, Huber AM, and Sim JH (2016). Influence of stimulation position on bone conduction sensitivity for bone condition hearing aids without skin penetration. International Journal of Audiology 55 (8): 439-446.

Dobrev I, Sim JH, Stenfelt S, Ihrle S, Gerig R, Pfiffner F, Eiber A, Huber AM, Röösli C. (2017). Sound wave propagation on the human skull surface with bone conduction stimulation. Hearing Research 355: 1-13.

Eeg-Olofsson M, Stenfelt S, Tjellström A, and Granström G (2008). Transmission of bone-conducted sound in the human skull measured by cochlear vibrations. International Journal of Audiology 47: 761-769.

Fisch U, May J, and Linder T (2008). Tympanoplasty, mastoidectomy and stapes surgery, second edition. Georg Thieme Verlag, Stuttgart, Germany.

Huber AM, Sim JH, Chatzimichalis M, Ullrich O, and Röösli C (2013). The Bonebridge; preclinical evaluation of a new transcutaenously-activated bone anchored hearing device. Hearing Research 301: 93-99.

Ito T, Röösli C, Kim CJ, Sim JH, Huber AM, and Probst R (2011). Bone conduction thresholds and skull vibration measured on the teeth during simulation at different sites on the human head. Audiology & Neurotology 16: 12-22.

McKnight CL, Doman DA, Brown JA, Bance M, and Adamson RB (2013). Direct measurement of the wavelength of sound waves in the human skull. J Acoust Soc Am. 133(1): 136-145.

Sim JH, Röösli C, Gerig R, Dalbert A, Fausch BC, Stenfelt S, and Huber AM (2014). Distribution of intra-cranial sound pressure during bone conduction stimulation. The 37th Association for Research in Otolaryngology Mid-Winter Meeting, San Diego, California, USA.

Stenfelt S and Goode RL (2005). Transmission properties of bone conducted sound: measurements in cadaver heads. J. Acoust. Soc. Am. 118: 2373-2391.

Figure1

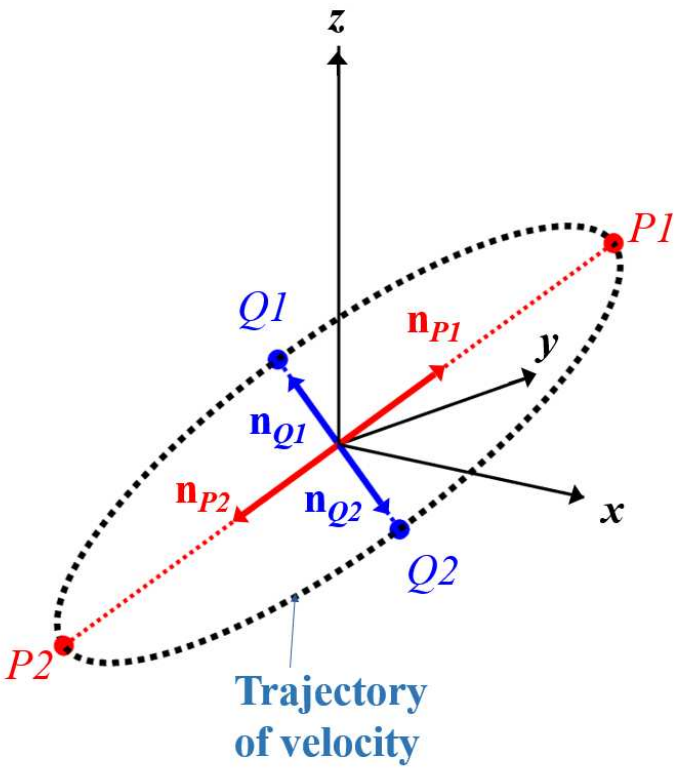

Fig. 1. Illustration of the trajectory of a 3D velocity vector **V** during one cycle, and the points of the maximum (*P*1 and *P*2) and minimum (*Q*1 and *Q*2) magnitudes, and corresponding directional vectors ($\mathbf{n}_{P1}$ and $\mathbf{n}_{P2}$ for the maximum magnitude and $\mathbf{n}_{Q1}$ and $\mathbf{n}_{Q2}$ for the minimum magnitude).

Figure2

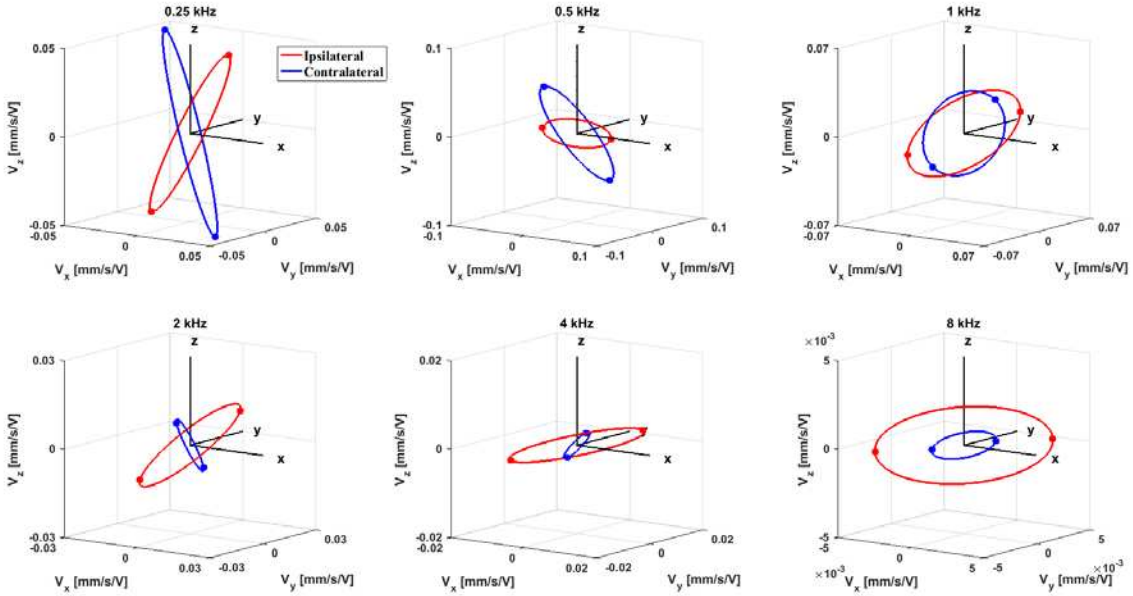

Fig. 2. The trajectories of the cochlear promonontory velocities during a cycle on the ipsilateral (red) and contralateral (blue) sides, at 0.25, 1, 2, 4 and 8 kHz. The spheres at each trajectory indicate the points of the maximum magnitude.

Figure3

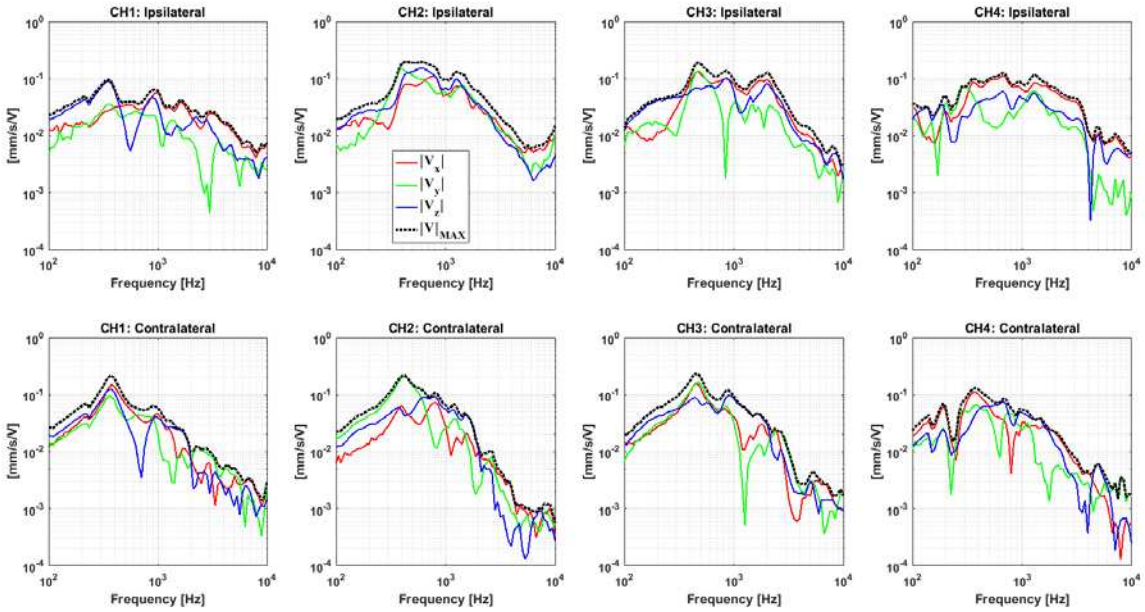

Fig. 3. The maximum magnitude (dotted black) of the cochlear promontory velocities in comparison with the magnitudes of the x- (red), y- (green), and z- (blue) components, for the ipsilateral (upper) and the contralateral (bottom) sides.

Figure4

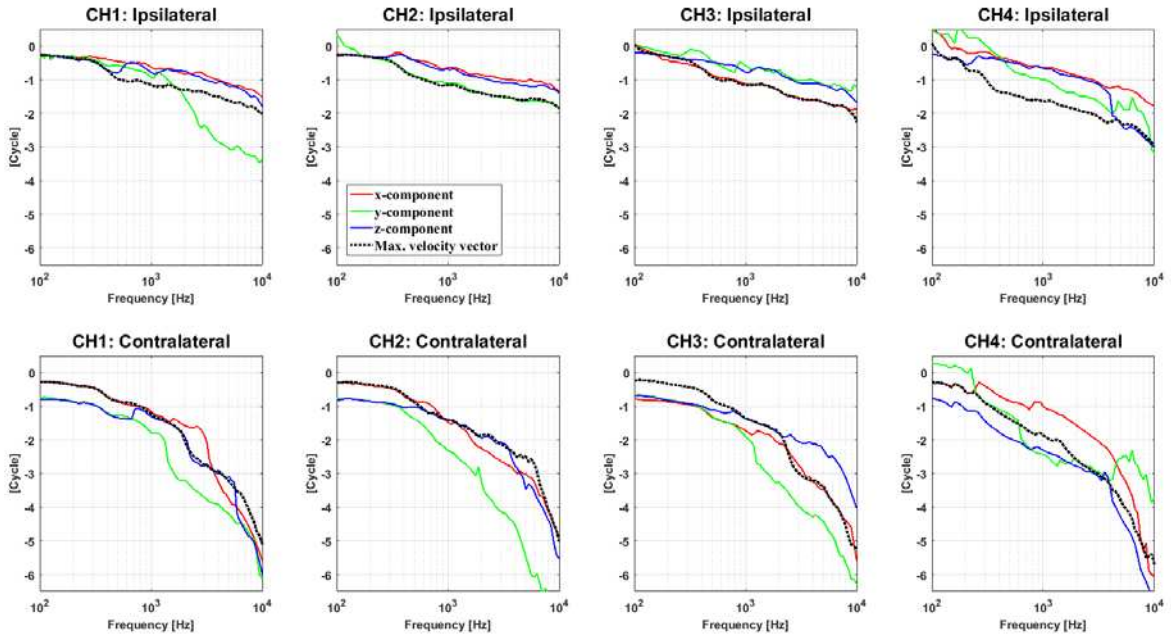

Fig. 4. The phases of the maximum velocity vector (dotted black) of the cochlear promontory velocities in comparison with the phases of the x- (red), y- (green), and z- (blue) components, for the ipsilateral (upper) and the contralateral (bottom) sides.

Figure5

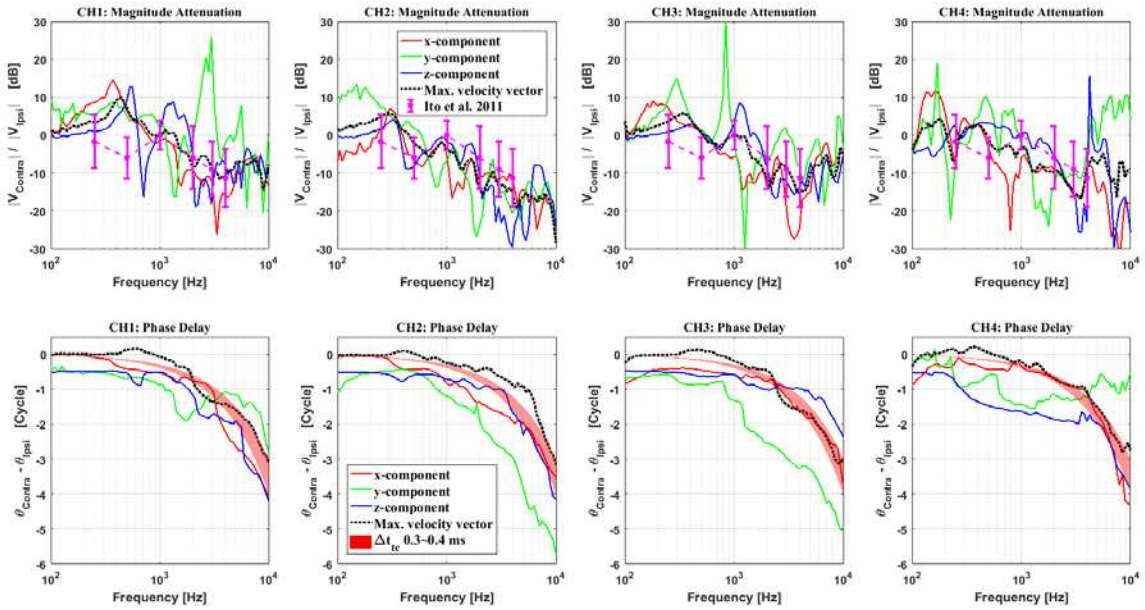

Fig. 5. The transcranial attenuation (upper) and phase delays of the contralateral side relative to the ipsilateral side, calculated from the x- (red), y- (green), and z- (blue) components, and maximum velocity vector (dotted black). The averages (AVG) and standard deviations (STD) of the interaural differences in audiometric thresholds reported by Ito et al. (2011) and expected phase delay with a transcranial time interval (Δt_{tc}) of 0.3~0.4 ms, as reported in the literature, are shown as well.

Figure6

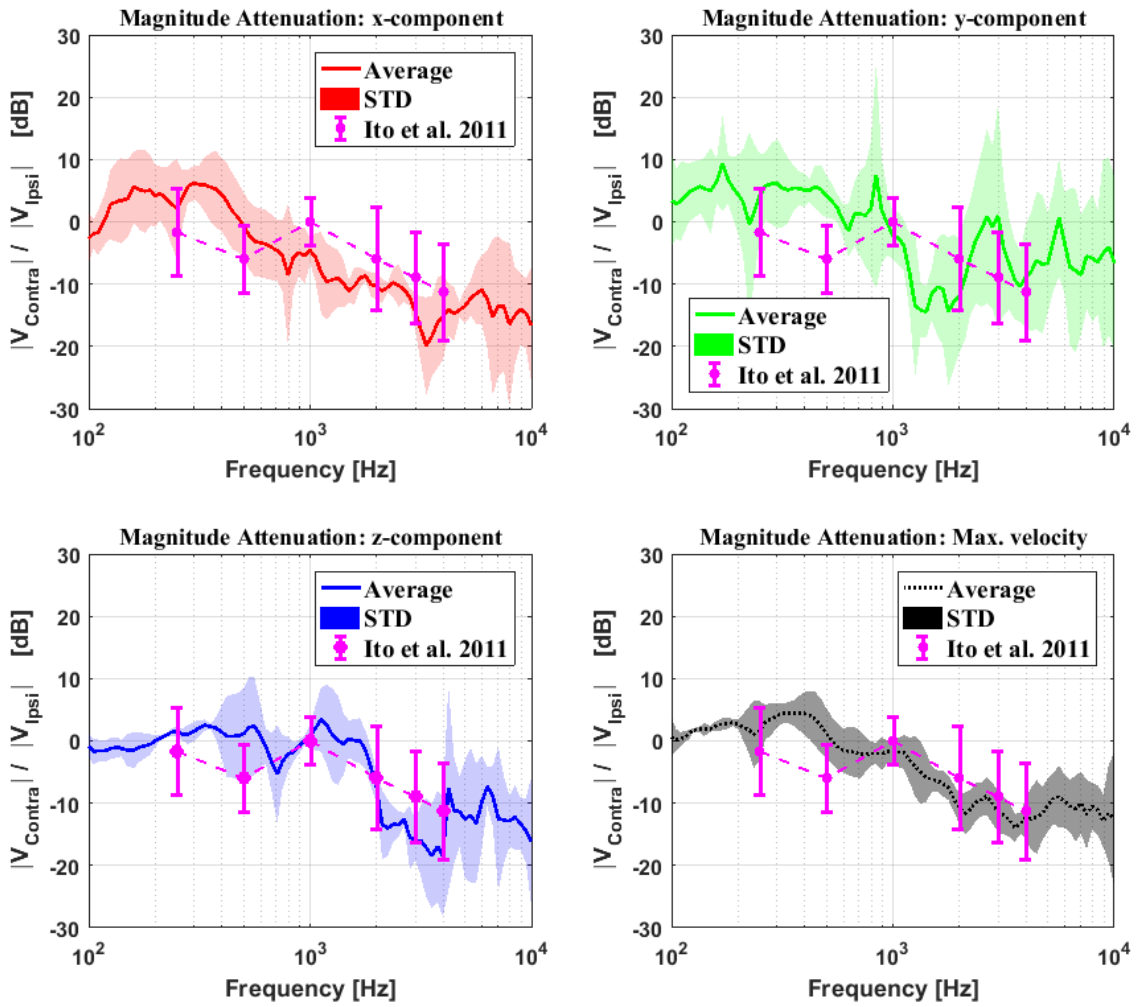

Fig. 6. The transcranial attenuation with the averages and standard deviations (STD) across four cadaver heads, in comparison with the interaural differences in audiometric thresholds reported by Ito et al. (2011).